

Universal Smoothed Score Functions for Generative Modeling

Saeed Saremi^{1, 2} Rupesh Kumar Srivastava³ Francis Bach⁴

¹UC Berkeley ²Prescient Design, Genentech, Roche ³NNAISENSE

⁴Inria, Ecole Normale Supérieure, PSL Research University

Abstract

We consider the problem of generative modeling based on smoothing an unknown density of interest in \mathbb{R}^d using factorial kernels with M independent Gaussian channels with equal noise levels introduced by [Saremi and Srivastava \(2022\)](#). First, we fully characterize the time complexity of learning the resulting smoothed density in \mathbb{R}^{Md} , called M-density, by deriving a universal form for its parametrization in which the score function is by construction permutation equivariant. Next, we study the time complexity of sampling an M-density by analyzing its condition number for Gaussian distributions. This spectral analysis gives a geometric insight on the “shape” of M-densities as one increases M . Finally, we present results on the sample quality in this class of generative models on the CIFAR-10 dataset where we report Fréchet inception distances (14.15), notably obtained with a single noise level on long-run fast-mixing MCMC chains.

1 Introduction

Smoothing a density with a kernel is a technique in nonparametric density estimation that goes back to [Parzen \(1962\)](#) at the birth of modern statistics. There has been a recent interest in estimating smoothed densities that are obtained by Gaussian convolution ([Saremi and Hyvärinen, 2019](#); [Goldfeld et al., 2020](#)), where instead of the random variable X the problem is to model the random variable $Y = X + \mathcal{N}(0, \sigma^2 I_d)$ based on a finite number of independent samples $\{x_i\}_{i=1}^n$ drawn from p_X . There is a subtle difference between this problem and the problem addressed by [Parzen \(1962\)](#). In the original problem (estimating p_X), the bandwidth of the Gaussian kernel σ is adjusted depending on the number of samples (typically tending to zero when the sample size goes to infinity). Here the kernel bandwidth σ is *fixed*. As one might expect, learning p_Y is simpler than learning p_X , but the problem is quite rich with deep connections to empirical Bayes and score matching as we highlight next.

Empirical Bayes formulated by [Robbins \(1956\)](#) is concerned with the problem of estimating the random variable X given a single noisy observation $Y = y$ assuming the noise model $p_{Y|X}$ is known. A classical result states that the least-squares estimator of X is the Bayes estimator:

$$\hat{x}(y) = \frac{\int xp(y|x)p(x)dx}{\int p(y|x)p(x)dx}.$$

But the remarkable result obtained in Robbin’s seminal paper is that the Bayes estimator can be written in closed form purely in terms of p_Y for a variety of noise models: the explicit knowledge of p_X is not required in this estimation problem. In addition, this dependency is only in terms of the *unnormalized* p_Y for all known empirical Bayes estimators, although this fact was not highlighted by [Robbins \(1956\)](#). For isotropic Gaussian the estimator takes the form¹

$$\hat{x}(y) = y + \sigma^2 g(y),$$

¹This result for Gaussian noise models was first derived by [Miyasawa \(1961\)](#) but has a rich history of its own; see [Raphan and Simoncelli \(2011\)](#) for a survey.

where $g(y) = \nabla \log p(y)$ is known in the literature as the score function (Hyvärinen, 2005).

This is the starting point in neural empirical Bayes (NEB) (Saremi and Hyvärinen, 2019), where the score function is parametrized using a neural network, arriving at the following learning objective

$$\mathcal{L}(\theta) = \mathbb{E}_{(x,y) \sim p(y|x)p(x)} \|x - \hat{x}_\theta(y)\|^2.$$

Algorithmically, NEB is attractive on two fronts: (i) the learning/estimation problem is reduced to the optimization of the least-squares denoising objective, where MCMC sampling is not required during learning, (ii) generative modeling is reduced to sampling p_Y which is better conditioned than sampling p_X (see Sec. 4) combined with the estimation of X which is a deterministic computation itself, referred to as walk-jump sampling (WJS).

The main problem with NEB, from the perspective of generative modeling (sampling p_X), is that we cannot sample from $p(x|y)$, and we do not have a control over how concentrated $p(x|y)$ is around its mean $\hat{x}(y) = \mathbb{E}[X|Y = y]$. A solution to this problem was formulated by Saremi and Srivastava (2022), where the noise model in NEB was replaced with a multimeasurement noise model (MNM):

$$p(\mathbf{y}|x) = \prod_{m=1}^M p(y_m|x),$$

where the bold-faced \mathbf{y} denotes the multimeasurement random variable $\mathbf{y} = (y_1, \dots, y_M)$. As we review in Sec. 2, the algorithmic attractions of NEB carry over to Gaussian MNMs with the added benefits that by simply increasing the number of measurements M , the posterior $p(x|\mathbf{y})$ automatically concentrates around its mean. Of particular interest is the case where the M noise levels are identical, therefore the M-density $p(\mathbf{y})$ is permutation invariant—this class of models is denoted by (σ, M) which is our focus in this paper.

1.1 Contributions

Our theoretical contributions are concerned with answering the following two questions:

- *What is the time complexity of learning M-densities?* We show that the M-densities associated with (σ, M) and (σ', M') can be mapped to each other if $\sigma/\sqrt{M} = \sigma'/\sqrt{M'}$. The permutation-invariant Gaussian M-densities are therefore grouped into universality classes $[\sigma_{\text{eff}}]$ where $\sigma_{\text{eff}} := \sigma/\sqrt{M}$. We arrive at a parametrization scheme for the score function associated with M-densities, called GPS, that is by construction permutation equivariant with respect to the permutation of the measurement indices. As a side effect of the GPS parametrization, we derive a single estimator of X given $\mathbf{Y} = \mathbf{y}$ instead of M (approximately equal) estimators by Saremi and Srivastava (2022).
- *What is the time complexity for sampling M-densities?* Knowing that M-densities are grouped into universality classes, the more subtle question is: which member has better mixing time properties? This is an important question to answer in understanding the generative modeling properties of M-densities. This question is a difficult one in its full generality, but to shed light on it we assume the original density p_X is a non-isotropic Gaussian, and we study the full spectrum of the corresponding M-density. The calculation gives insight on the “geometry” of M-densities as one increases M . See Fig. 1 for a schematic.

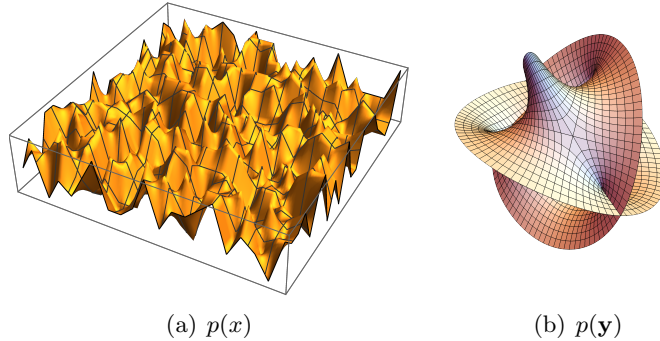


Figure 1: (*The geometry of M -densities*) (a) Schematic of a complex density in \mathbb{R}^d ($d = 2$). (b) The plot represents the manifold associated with the corresponding permutation-invariant M -density in \mathbb{R}^{Md} . The schematic is meant to capture the fact that the M -density is symmetric and it is smoother than the original density.

Experiments are focused on the generative modeling problem on the CIFAR-10 dataset (Krizhevsky et al., 2009). This dataset has proved to be challenging for generative models due to the diversity of image classes present. The performance of the generative models are measured in FID score (Heusel et al., 2017) (the lower score is better). As an example, a sophisticated model like BigGAN (Brock et al., 2019), in the generative adversarial networks (Goodfellow et al., 2014) family, achieves the FID score of 14.73. Our framework is based on a simple denoising objective with a single noise level, yet despite its simple structure we can achieve the FID score of **14.15**, which is remarkable in this class of models. Our experimental results question the current perception in the field that denoising models with a single noise level cannot be good generative models.

1.2 Related Work

The work directly related to this paper is by Saremi and Srivastava (2022) who introduced a generative modeling framework based on smoothing an unknown density of interest with factorial kernels with M channels. Our focus here is on Gaussian kernels and our main contribution is to show any single measurement model $(\sigma, 1)$ can be mapped to a multimeasurement one $(\sigma\sqrt{M}, M)$; no additional learning is required. In particular, in our work the neural network inputs are in \mathbb{R}^d as opposed to \mathbb{R}^{Md} in the earlier work. In addition, there were open questions regarding the role M in the sampling complexity in the earlier work that this work aims to address.

At a broader level, this work is related to the research on denoising density models, a class of probabilistic models that grew from the literature on score matching and denoising autoencoders (Hyvärinen, 2005; Vincent, 2011; Alain and Bengio, 2014; Saremi et al., 2018). These models were not successful in the past on challenging generative modeling tasks, e.g. on the CIFAR-10 dataset, which in turn led to research on denoising objectives with multiple noise levels (Song and Ermon, 2019). In our experiments, we revisit denoising density models with a single noise level. In particular, our experimental results question the current perception in the field around the topic of single vs. multiple noise scales. As an example, we point out that the FID score in this paper (14.15) is significantly lower than the one reported by Song and Ermon (2019) (25.32) which was obtained using annealed Langevin MCMC with multiple noise scales. Also see Jain and Poole (2022) for a recent work on score-based generative modeling with a single noise level.

2 Background

In this section, we review smoothing with factorial kernels and their use for generative modeling. We refer to [Saremi and Srivastava \(2022\)](#) for more details and references.

Factorial Kernels. Smoothing a density with a (Gaussian) kernel is a well-known technique in nonparametric density estimation that goes back to [Parzen \(1962\)](#); see [Hastie et al. \(2009\)](#) for a general introduction to kernels. Given a density p_X in \mathbb{R}^d one can construct a smoother density p_Y in \mathbb{R}^d by convolving it with a positive-definite kernel $k : \mathbb{R}^d \times \mathbb{R}^d \rightarrow \mathbb{R}$:

$$p(y) = \int k(x, y)p(x)dx.$$

In this paper we only consider (translation-invariant) isotropic Gaussian kernels, where one can also have a dual perspective on the kernel as the conditional density $k(x, y) = p(y|x)$, where

$$p(y|x) = \frac{1}{Z(\sigma)} \exp\left(-\frac{\|y-x\|^2}{2\sigma^2}\right) =: \mathcal{N}(y; x, \sigma^2 I_d).$$

Here $Z(\sigma)$ is the partition function associated with the isotropic Gaussian. From this angle, smoothing a density with an isotropic Gaussian kernel can also be expressed in terms of random variables as follows:

$$Y = X + \mathcal{N}(0, \sigma^2 I_d).$$

A factorial kernel is a generalization of the above where the kernel $k(x, y)$ takes the following factorial form with M kernel components:

$$k(x, \mathbf{y}) = \prod_{m=1}^M k(x, y_m), \text{ where } \mathbf{y} = (y_1, \dots, y_M).$$

For isotropic Gaussian kernels this is equivalent to $Y_m = X + \mathcal{N}(0, \sigma^2 I_d)$ for $m \in [M]$ (with independent Gaussians). The kernel $k(x, \mathbf{y})$ is referred to as multimeasurement noise model (MNM).² The result of the convolution with a Gaussian MNM is referred to as Gaussian M-density associated with the random variable $\mathbf{Y} = (Y_1, \dots, Y_M)$ which takes values in \mathbb{R}^{Md} . Given $\{x_i\}_{i=1}^n$, independent draws from the density p_X , we are interested in estimating the associated M-density for a given fixed noise level σ .

Multimeasurement Bayes Estimators. How can we go about estimating the M-density? One approach is to formulate it as a learning problem ([Vapnik, 1999](#)) by parametrizing the M-density (say with a neural network) and devising an appropriate learning objective. For $M = 1$, the learning objective is given by:

$$\mathcal{L}(\theta) = \mathbb{E}_{(x,y) \sim p(x)p(y|x)} \|x - \hat{x}_\theta(y)\|^2, \tag{1}$$

where $\hat{x}_\theta(y)$ is a parametrization of the Bayes estimator of X given $Y = y$ in terms of $p_\theta(y)$. This approach heavily relies on the fact that the Bayes estimator $\hat{x}(y)$ can indeed be expressed in closed form in terms of $p(y)$, which is a key result at the heart of empirical Bayes ([Robbins, 1956](#)). In addition, for Gaussian kernels, the Bayes estimator can be expressed in terms of the score function

²One can view smoothing with a factorial kernel in the context of a communication system ([Shannon, 1948](#)) with M independent noise channels, i.e., given $X = x$ samples (y_1, \dots, y_m) are obtained by adding M independent isotropic Gaussian noise to x .

$\nabla \log p(y)$, a result that goes back to Miyasawa (1961), therefore for learning $p(y)$ one can ignore its partition function (Saremi and Hyvärinen, 2019). This key result in the empirical Bayes literature was extended by Saremi and Srivastava (2022) to Poisson and Gaussian MNMs, where for Gaussian MNMs, $\hat{x}(\mathbf{y}) = \mathbb{E}[X|\mathbf{Y} = \mathbf{y}]$ takes the following form:

$$\hat{x}(\mathbf{y}) = y_m + \sigma^2 \nabla_m \log p(\mathbf{y}), \quad (2)$$

where $m \in [M]$ is an arbitrary measurement index (the result is invariant to this choice). Note that the Bayes estimator $\hat{x}(\mathbf{y})$ only depends on the score function associated with the M-density, therefore one can use Eq. 1 as the objective for learning the energy/score function associated with the M-density by simply replacing y with $\mathbf{y} = (y_1, \dots, y_M)$.

Walk-Jump Sampling. Following learning the score function $\nabla \log p(\mathbf{y})$, one can use Langevin MCMC to draw exact samples from $p(\mathbf{y})$. For $M = 1$ the density $p(y)$ is smoother than $p(x)$ and MCMC is assured to mix faster. What about drawing samples from $p(x)$? The idea behind walk-jump sampling (WJS) is that one can indeed use the score function $\nabla \log p(y)$ to estimate X thus arriving at approximate samples from $p(x)$ (Saremi and Hyvärinen, 2019). There is clearly a trade-off here: by decreasing σ the estimate of X becomes more and more accurate (WJS becomes more and more exact) but this comes at the cost of sampling a less smooth $p(y)$ where MCMC has a harder time. On the surface, what is intriguing about M-density is that one can keep σ to be “large” and still have a control on generating exact samples from $p(x)$ by simply increasing M . The full picture on the effects of increasing M is more complex which we discuss after our analysis in Sec. 4.

3 Universal M-densities

In this section we derive a general expression for the M-density $p(\mathbf{y})$ and the score function $\nabla \log p(\mathbf{y})$ for Gaussian MNMs with equal noise levels σ . For equal noise levels, the M-density (resp. score function) is permutation invariant (resp. equivariant) under the permutation of measurement indices (Saremi and Srivastava, 2022). However, it is not clear a priori how this invariance/equivariance should be reflected in the parametrization. The calculation below clarifies this issue, where we arrive at a general permutation invariant (resp. equivariant) parametrization for the M-density (resp. score function) in which the empirical mean of the M measurements

$$\bar{y} = M^{-1} \sum_{m=1}^M y_m$$

plays a central role. We start with a rewriting of the log p.d.f. of the factorial kernel:

$$\begin{aligned} -2\sigma^2 \log p(\mathbf{y}|x) &= \sum_{m=1}^M \|y_m - x\|^2 + C \\ &= M\|x\|^2 - 2\langle \sum_{m=1}^M y_m, x \rangle + \sum_{m=1}^M \|y_m\|^2 + C \\ &= M(\|x\|^2 - 2\langle \bar{y}, x \rangle + \overline{\|y\|^2}) + C \\ &= M(\|x - \bar{y}\|^2 + \overline{\|y\|^2} - \|\bar{y}\|^2) + C, \end{aligned} \quad (3)$$

where $C = 2\sigma^2 M \log Z(\sigma)$ and $\overline{\|y\|^2}$ is short for

$$\overline{\|y\|^2} = M^{-1} \sum_{m=1}^M \|y_m\|^2.$$

Now, we view the smoothing kernel $p(\mathbf{y}|x)$ as a Gaussian distribution over X centered at \bar{y} :

$$\begin{aligned} \log p(\mathbf{y}) &= \log \int p(\mathbf{y}|x)p(x)dx \\ &= \log \int \mathcal{N}(x; \bar{y}, \sigma_{\text{eff}}^2 I_d) p(x) dx + \frac{\|\bar{y}\|^2 - \overline{\|y\|^2}}{2\sigma_{\text{eff}}^2} + C' \\ &= \log \mathbb{E}_{X \sim \mathcal{N}(\bar{y}, \sigma_{\text{eff}}^2 I_d)} [p(X)] + \frac{\|\bar{y}\|^2 - \overline{\|y\|^2}}{2\sigma_{\text{eff}}^2} + C', \end{aligned} \quad (4)$$

where $\sigma_{\text{eff}} := \sigma/\sqrt{M}$, and $C' = \log Z(\sigma_{\text{eff}}) - M \log Z(\sigma)$. Note that the first term above is a function of \bar{y} for any distribution p_X , therefore the energy function $f(\mathbf{y})$ takes the following form:

$$f(\mathbf{y}) = \frac{1}{2\sigma_{\text{eff}}^2} \left(\overline{\|y\|^2} - \|\bar{y}\|^2 \right) + \varphi(\bar{y}). \quad (5)$$

Next we consider the functional form for the score function $\mathbf{g}(\mathbf{y}) = -\nabla f(\mathbf{y})$. Taking gradients leads to:

$$g_m(\mathbf{y}) = \frac{1}{2\sigma_{\text{eff}}^2} (2\bar{y}/M - 2y_m/M) - \nu(\bar{y})/M,$$

where $\nu = \nabla \varphi$. The expression above is written more compactly (to be used below) as

$$\sigma^2 g_m(\mathbf{y}) = (\bar{y} - y_m) - \sigma_{\text{eff}}^2 \cdot \nu(\bar{y}). \quad (6)$$

Finally, the expression for the Bayes estimator $\hat{x}(\mathbf{y})$ is derived (combine [Eq. 2](#) and [Eq. 6](#)):

$$\hat{x}(\mathbf{y}) = \bar{y} - \sigma_{\text{eff}}^2 \cdot \nu(\bar{y}). \quad (7)$$

3.1 GPS Parametrization

The results above leads to the following parametrization for the score function:

Definition 1 (GPS). *The GPS parametrization of the score function associated with the M -density for (σ, M) models is given by (replace ν with ν_θ in [Eq. 6](#))*

$$\sigma^2 g_m(\mathbf{y}; \theta) = (\bar{y} - y_m) - \sigma_{\text{eff}}^2 \cdot \nu_\theta(\bar{y}), \quad (8)$$

where $\nu_\theta : \mathbb{R}^d \rightarrow \mathbb{R}^d$ is either parametrized directly/explicitly or indirectly/implicitly by parametrizing the function $\varphi_\theta : \mathbb{R}^d \rightarrow \mathbb{R}$. In the later case, ν_θ is derived as follows:

$$\nu_\theta = \nabla \varphi_\theta.$$

The GPS parametrization has two important properties captured by the following propositions:

Proposition 1 (Permutation equivariance property of GPS). *The score function parametrized in GPS is permutation equivariant:*

$$\mathbf{g}_\theta(\pi(\mathbf{y})) = \pi(\mathbf{g}_\theta(\mathbf{y})), \quad (9)$$

where $\pi : [M] \rightarrow [M]$ is a permutation of the noise/measurement channels whose action on $\mathbf{y} = (y_1, \dots, y_M)$ and $\mathbf{g} = (g_1, \dots, g_M)$ is to permute the measurement channels:

$$\pi((y_1, \dots, y_M)) = (y_{\pi(1)}, \dots, y_{\pi(M)}).$$

$$\pi((g_1, \dots, g_M)) = (g_{\pi(1)}, \dots, g_{\pi(M)}).$$

Proof. The proof is straightforward since \bar{y} in GPS is permutation invariant. \square

The naming GPS has been derived from the statement of [Proposition 1](#): \mathbf{g}_θ is a permutation-equivariant score function. Informally (alluding to GPS as the “global positioning system”), in the GPS parametrization, the “coordinates” of the M-density manifold in high dimensions is validly encoded in the sense of respecting its permutation invariance. This important symmetry is broken in the MDAE parametrization studied in ([Saremi and Srivastava, 2022](#)).

In addition, in GPS, the Bayes estimator ([Eq. 7](#)) takes the following parametric form:

$$\hat{x}_\theta(\mathbf{y}) = \bar{y} - \sigma_{\text{eff}}^2 \cdot \nu_\theta(\bar{y}), \quad (10)$$

where the measurement index m does not appear in the final expression—this is in contrast to the parametrization studied by [Saremi and Srivastava \(2022\)](#).

3.2 GPS is Universal

Before formalizing the universality of the GPS parametrization in [Proposition 2](#) below, we define the notion of universality classes associated with M-densities:

Definition 2 (M-density Universality Classes). *We define the universality class $[\sigma_{\text{eff}}]$ as the set of all (σ, M) models*

$$[\sigma_{\text{eff}}] := \{(\sigma_1, M_1), (\sigma_2, M_2), \dots\},$$

such that for all $(\sigma_i, M_i) \in [\sigma_{\text{eff}}]$:

$$\frac{\sigma_i}{\sqrt{M_i}} = \sigma_{\text{eff}}.$$

In particular, the models $\{(\sigma_{\text{eff}}\sqrt{M}, M) : M \in \mathbb{N}\}$ belong to the universality class $[\sigma_{\text{eff}}]$.

The universality property of GPS is captured by the following proposition:

Proposition 2 (The universal property of GPS). *For any parameter θ , all (σ, M) models that belong to the same universality class and parametrized by GPS are identical in the sense that they incur the same loss*

$$\mathcal{L}_{\sigma, M}(\theta) = \mathcal{L}_{\sigma', M'}(\theta) \text{ if } \frac{\sigma}{\sqrt{M}} = \frac{\sigma'}{\sqrt{M'}}, \quad (11)$$

where

$$\mathcal{L}_{\sigma, M}(\theta) = \mathbb{E}_{(x, \mathbf{y}) \sim p(x)p(\mathbf{y}|x)} \|x - \hat{x}_\theta(\mathbf{y})\|^2.$$

Proof. Using [Eq. 10](#), we have

$$\mathcal{L}_{\sigma, M}(\theta) = \mathbb{E}_{(x, \mathbf{y}) \sim p(x)p(\mathbf{y}|x)} \|x - \bar{y} + \sigma_{\text{eff}}^2 \cdot \nu_{\theta}(\bar{y})\|^2. \quad (12)$$

Note that $x - \bar{y}$ has the same law as $\mathcal{N}(0, \sigma_{\text{eff}}^2 I_d)$, where $\sigma_{\text{eff}} = \sigma/\sqrt{M}$. Therefore, the learning objective has the interpretation that ν_{θ} makes predictions on the residual noise left in the empirical mean of the noisy measurements since $\bar{y} = x + \bar{\gamma}$, where $\bar{\gamma} = M^{-1} \sum_{m=1}^M \gamma_m$ and γ_m are independent samples from $\mathcal{N}(0, \sigma^2 I_d)$. This observation can be made explicit by rewriting $\mathcal{L}_{\sigma, M}(\theta)$ as:

$$\mathbb{E}_{x \sim p(x), \{\gamma_m \sim \mathcal{N}(0, \sigma^2 I_d)\}_{m=1}^M} \|\bar{\gamma} - \sigma_{\text{eff}}^2 \cdot \nu_{\theta}(x + \bar{\gamma})\|^2.$$

The statement of the proposition follows since $\bar{\gamma}$ has the same law as $\mathcal{N}(0, \sigma_{\text{eff}}^2 I_d)$ for (σ, M) and (σ', M') models since they are both in the universality class $[\sigma_{\text{eff}}]$. \square

Corollary 1. *The laws of $\hat{x}_{\theta}(\mathbf{Y})$ are identical for all (σ, M) models in the same universality class and for all θ in the GPS parametrization.*

Proof. In the GPS parametrization $\hat{x}_{\theta}(\mathbf{Y}) = \bar{Y} - \sigma_{\text{eff}}^2 \cdot \nu_{\theta}(\bar{Y})$ ([Eq. 10](#)). The proof then follows from the proof in the above proposition since \bar{Y} has the same law as $X + \mathcal{N}(0, \sigma_{\text{eff}}^2 I_d)$ for all models in $[\sigma_{\text{eff}}]$. \square

4 On the shape of M-densities

In the previous section we established that (σ, M) models in the same universality class $[\sigma_{\text{eff}}]$ ([Definition 2](#)) are equivalent in the sense formalized in [Proposition 2](#) and [Corollary 1](#). In this section, we switch our focus to how difficult it is to sample universal M-densities. In particular, we formalize the intuition that $(\sigma_{\text{eff}}\sqrt{M}, M) \in [\sigma_{\text{eff}}]$ become more spherical by increasing M . The analysis also sheds some light on the geometry of M-densities as one increases M (for a fixed σ).

An important parameter characterizing the shape of log-concave densities is the condition number denoted by κ which measures how elongated the density is ([Cheng et al., 2018](#), Section 1.4.1). The condition number appears in the mixing time analysis of log-concave densities, e.g. in the form κ^2 in ([Cheng et al., 2018](#)). Intuitively, for poorly conditioned densities one has to use a small step size and that will lead to long mixing times.

For Gaussian densities

$$p(x) = \mathcal{N}(x; \mu, \Sigma),$$

the condition number denoted by κ is given by

$$\kappa = \lambda_{\max}(F)/\lambda_{\min}(F), \quad (13)$$

where $\lambda(F)$ denotes the spectrum of the inverse covariance matrix $F := \Sigma^{-1}$.

Next, we study the full spectrum of the corresponding M -density and give an expression for the condition number of (σ, M) models. We assume without loss of generality a basis in \mathbb{R}^d where the density is centered at $\mu = 0$ and the covariance matrix is diagonalized: $\Sigma_{ij} = \tau_i^2 \delta_{ij}$. Therefore,

$$p(x) = \prod_{i=1}^d \frac{1}{Z(\tau_i)} \exp\left(-\frac{x_i^2}{2\tau_i^2}\right),$$

and $\kappa = \tau_{\max}^2/\tau_{\min}^2$. Next we study the condition number for (σ, M) models. The case $M = 1$ is simple since

$$F = (\Sigma + \sigma^2 I_d)^{-1},$$

therefore

$$\kappa(\sigma, 1) = \frac{\tau_{\max}^2 + \sigma^2}{\tau_{\min}^2 + \sigma^2}. \quad (14)$$

We switch to studying the full spectrum of the covariance matrix for (σ, M) models where $M > 1$. We start with the expression for $p(\mathbf{y})$ given below up to a normalizing constant for the general M-density defined by the noise levels $(\sigma_1, \sigma_2, \dots, \sigma_M)$:

$$\begin{aligned} p(\mathbf{y}) &\propto \int \prod_{m=1}^M \mathcal{N}(x; y_m, \sigma_m^2 I_d) \cdot \mathcal{N}(x; 0, \Sigma) dx \\ &\propto \prod_{i=1}^d \int \exp\left(-\sum_{m=1}^M \frac{(y_{mi} - x_i)^2}{2\sigma_m^2} - \frac{x_i^2}{2\tau_i^2}\right) dx_i \\ &= \prod_{i=1}^d \int \exp\left(-\frac{(x_i - \alpha_i)^2}{2\beta_i^2} - \gamma_i\right) dx_i \\ &\propto \prod_{i=1}^d \exp(-\gamma_i). \end{aligned} \quad (15)$$

The expressions for α_i , β_i , and γ_i are given next by completing the square via matching second, first and zeroth derivative (in that order) of the left and right hand sides below

$$-\sum_{m=1}^M \frac{(y_{mi} - x_i)^2}{2\sigma_m^2} - \frac{x_i^2}{2\tau_i^2} = -\frac{(x_i - \alpha_i)^2}{2\beta_i^2} - \gamma_i \quad (16)$$

evaluated at $x_i = 0$. The following three equations follow:

$$\frac{1}{\beta_i^2} = \sum_{m=1}^M \frac{1}{\sigma_m^2} + \frac{1}{\tau_i^2}, \quad (17)$$

$$\frac{\alpha_i}{\beta_i^2} = \sum_{m=1}^M \frac{y_{mi}}{\sigma_m^2} \Rightarrow \alpha_i = \omega_i^2 \sum_{m=1}^M \frac{y_{mi}}{\sigma_m^2}, \quad (18)$$

$$-\frac{\alpha_i^2}{2\beta_i^2} - \gamma_i = -\sum_{m=1}^M \frac{y_{mi}^2}{2\sigma_m^2} \Rightarrow \gamma_i = \sum_{m=1}^M \frac{y_{mi}^2}{2\sigma_m^2} - \frac{1}{2}\omega_i^2 \left(\sum_{m=1}^M \frac{y_{mi}}{\sigma_m^2}\right)^2, \quad (19)$$

where

$$\omega_i^2 := \left(\sum_{m=1}^M \frac{1}{\sigma_m^2} + \frac{1}{\tau_i^2}\right)^{-1}. \quad (20)$$

Therefore the energy function associated with the random variable \mathbf{y} is given by:

$$f(\mathbf{y}) = \sum_m \frac{\|y_m\|^2}{2\sigma_m^2} - \frac{1}{2} \sum_{i=1}^d \omega_i^2 \left(\sum_{m=1}^M \frac{y_{mi}}{\sigma_m^2}\right)^2. \quad (21)$$

The energy function can be written more compactly by introducing the matrix \mathbf{F} :

$$f(\mathbf{y}) = \frac{1}{2} \langle \mathbf{y}, \mathbf{F} \mathbf{y} \rangle, \quad (22)$$

$$\mathbf{F}_{mi,m'i'} = [\sigma_m^{-2}(1 - \omega_i^2 \sigma_m^{-2}) \delta_{mm'} - \omega_i^2 \sigma_m^{-2} \sigma_{m'}^{-2}(1 - \delta_{mm'})] \delta_{ii'}.$$

In words, the $Md \times Md$ dimensional matrix \mathbf{F} is block diagonal with d blocks of size $M \times M$. The blocks themselves capture the interactions between different measurements indexed by m and m' . To study the spectrum of the covariance matrix, we next focus on (σ, M) models, i.e., the permutation-invariant case where $\sigma_m = \sigma$ for all $m \in [M]$:

$$\mathbf{F}_{mi,m'i'} = [\sigma^{-2}(1 - \omega_i^2 \sigma^{-2}) \delta_{mm'} - \omega_i^2 \sigma^{-4}(1 - \delta_{mm'})] \delta_{ii'}, \quad (23)$$

$$\omega_i^2 = (M\sigma^{-2} + \tau_i^{-2})^{-1}.$$

The $M \times M$ blocks of the matrix \mathbf{F} have the form:

$$\mathbf{F}_i = \begin{pmatrix} a_i & b_i & \dots & b_i \\ b_i & a_i & \dots & b_i \\ \vdots & & \ddots & \\ b_i & b_i & \dots & a_i \end{pmatrix},$$

where

$$a_i = \sigma^{-2}(1 - \omega_i^2 \sigma^{-2}), \quad (24)$$

$$b_i = -\omega_i^2 \sigma^{-4}. \quad (25)$$

It is straightforward to find the M eigenvalues of the matrix \mathbf{F}_i :

- $M - 1$ degenerate eigenvalues equal to $a_i - b_i$ corresponding to the eigenvectors

$$\{(1, -1, 0, \dots, 0)^\top, (1, 0, -1, \dots, 0)^\top, \dots, (1, 0, 0, \dots, -1)^\top\},$$

- one eigenvalue equal to $a_i + (M - 1)b_i$ corresponding to the eigenvector $(1, 1, \dots, 1)^\top$.

Since $a_i > 0$, $b_i < 0$ we arrive at:

$$\lambda_{\max}(\mathbf{F}) = a_i - b_i = \sigma^{-2}$$

which is $(M - 1)d$ degenerate on the full matrix \mathbf{F} . The remaining d eigenvalues are given by

$$\lambda_i = a_i + (M - 1)b_i = \sigma^{-2}(1 - M\omega_i^2 \sigma^{-2}), \quad (26)$$

the smallest of which is given by

$$\lambda_{\min}(\mathbf{F}) = \sigma^{-2}(1 - M\sigma^{-2}\omega_{\max}^2) = \sigma^{-2} \left(1 - M\sigma^{-2} \frac{1}{M\sigma^{-2} + \tau_{\max}^{-2}} \right) = \frac{\sigma^{-2}}{1 + M\sigma^{-2}\tau_{\max}^2}. \quad (27)$$

It follows:

$$\kappa(\sigma, M) = \lambda_{\max}(\mathbf{F}) / \lambda_{\min}(\mathbf{F}) = 1 + M\sigma^{-2}\tau_{\max}^2. \quad (28)$$

5 Experiments

We conducted experiments on the CIFAR-10 dataset (Krizhevsky et al., 2009) of 32×32 color images from 10 classes. The goal of these experiments is to empirically study the results of sampling from GPS models in the same universality class as implied by our theoretical analysis in Sec. 3.

Training. ν_θ (from Eq. 10) was parameterized using the “U-Net” used in recent work on generative modeling on this dataset (Dhariwal and Nichol, 2021). We set $\sigma_{\text{eff}} = 0.25$, by choosing $\sigma = 1$ and $M = 16$ for training the network. Similar to the MDAE parametrization from Saremi and Srivastava (2022), learning essentially involves training a denoising autoencoder with a mean squared loss. For optimization, the Adagrad optimizer (Duchi et al., 2011) was used with a batch size of 128 and maximum 400 epochs of training. The learning rate was initialized 1×10^{-6} and scheduled to linearly increase to 1.5 over 1×10^6 updates (though training terminated earlier). During training, the FID score (Heusel et al., 2017) computed using samples from 125 parallel MCMC chains (400 samples each, resulting in 50,000 samples total) was monitored at regular intervals, and the model with the lowest FID score was selected as a form of early stopping.

Sampling Results. Our sampling algorithm is based on the walk-jump sampling (Saremi and Hyvärinen, 2019) that samples noisy data using the learned score function with Langevin MCMC (walk) together with the Bayes estimator of clean data (jump). For Langevin MCMC we considered three different algorithms (Sachs et al., 2017; Cheng et al., 2018; Shen and Lee, 2019). We settled on the algorithm by Sachs et al. (2017) early on as it was more reliable in the small-scale experiments that we performed (see Fig. 3(e) for a visual comparison to the randomized midpoint method by Shen and Lee (2019)). We set the step size $\delta = \sigma/2$ for all (σ, M) models and did extensive experiments on tuning the friction parameter. The results are shown in Fig. 2 where the FID score is obtained averaged over 5 random seeds. In the algorithm by Sachs et al. (2017) the friction parameter γ only shows up in the form $\gamma_{\text{eff}} = \gamma \cdot \delta$ which we call effective friction. This is especially important in our model since step sizes vary greatly between different (σ, M) models. The best results were obtained for $(0.25, 1)$ model with the FID of **14.15**. In addition, our results in Fig. 3 are remarkable in qualitatively demonstrating fast mixing in long-run MCMC chains, where diverse classes are visited in a single chain: such fast-mixing MCMC chains on CIFAR-10 have not been reported in the literature.

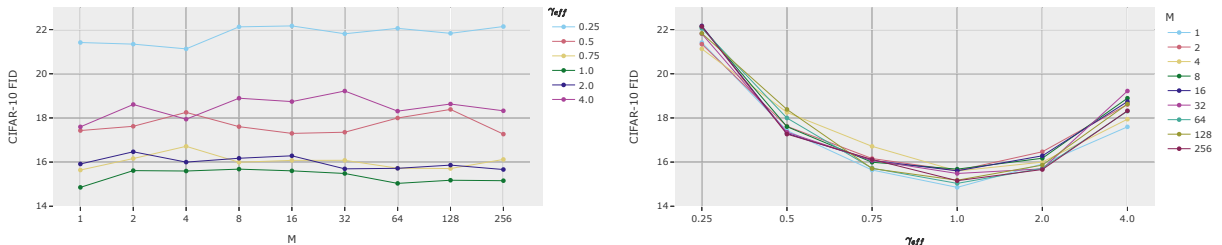


Figure 2: CIFAR-10 FID scores obtained when tuning the value of γ_{eff} for various values of M , for a model trained with $\sigma_{\text{eff}} = 0.25$.



(a) $(1/4, 1)$, $\delta = 1/8$, $\gamma = 8$



(b) $(1, 16)$, $\delta = 1/2$, $\gamma = 2$



(c) $(2, 64)$, $\delta = 1$, $\gamma = 1$



(d) $(4, 256)$, $\delta = 2$, $\gamma = 0.5$



(e) $(1, 16)$, $\delta = 1/2$, $\gamma = 2$

Figure 3: Examples of long-run MCMC chains on CIFAR-10 dataset for (σ, M) models in the $[\sigma_{\text{eff}} = 0.25]$ universality class. **Each panel represents a single MCMC chain.** Only 20 steps are taken per image, starting from noise, a total of 10 K steps (viewed left-to-right, top-to-bottom). We set $\delta = \sigma/2$, and we set the friction γ from [Sachs et al. \(2017\)](#), panels (a)-(d), such that $\gamma_{\text{eff}} := \gamma\delta = 1$. In the bottom panel we show the performance of randomized midpoint method ([Shen and Lee, 2019](#)) used for Langevin MCMC in the walk-jump sampling. The random seed is fixed across runs. Best seen zoomed on a computer screen.

6 Conclusion

This work was primarily concerned with the theoretical understanding of smoothing methods using factorial kernels proposed by [Saremi and Srivastava \(2022\)](#), where in particular we focused on the permutation-invariant case in which the model is defined by a single noise scale. We showed such models are grouped into universality classes in which the densities can be easily mapped to each other, and we introduced the GPS parametrization to utilize that. Theoretically, the models that belong to the same universality class should have very different sampling properties and we had an analysis of that here, focused on studying the condition number.

Our experimental results on CIFAR-10 were surprising on two fronts: (i) We achieved low FID scores which have been argued to be not feasible for denoising models with a single noise scale. In fact, the research on generative models based on denoising autoencoders (DAE) came to a halt around 2014 with the invention of GANs ([Goodfellow et al., 2014](#)), and we were ourselves surprised by a simple model such as $(0.25, 1)$ outperforming BigGAN ([Brock et al., 2019](#)) on the CIFAR-10 challenge. Note that, $(0.25, 1)$ is essentially a DAE with an empirical Bayes interpretation ([Saremi and Hyvärinen, 2019](#)). (ii) We also found it surprising that our experimental results did not show any benefit for larger M models, but that needs more investigation in future research. In particular, there might exist more “clever samplers” that need to be invented for exploiting the structure of (σ, M) models.

Acknowledgement

We would like to thank Ruoqi Shen for communication regarding their randomized midpoint method.

References

- Alain, G. and Bengio, Y. (2014). What regularized auto-encoders learn from the data-generating distribution. *Journal of Machine Learning Research*, 15(1):3563–3593.
- Brock, A., Donahue, J., and Simonyan, K. (2019). Large scale GAN training for high fidelity natural image synthesis. In *International Conference on Learning Representations*.
- Cheng, X., Chatterji, N. S., Bartlett, P. L., and Jordan, M. I. (2018). Underdamped Langevin MCMC: A non-asymptotic analysis. In *Conference on Learning Theory*, pages 300–323.
- Dhariwal, P. and Nichol, A. (2021). Diffusion models beat gans on image synthesis. *Advances in Neural Information Processing Systems*, 34:8780–8794.
- Duchi, J., Hazan, E., and Singer, Y. (2011). Adaptive subgradient methods for online learning and stochastic optimization. *Journal of Machine Learning Research*, 12(7).
- Goldfeld, Z., Greenewald, K., Niles-Weed, J., and Polyanskiy, Y. (2020). Convergence of smoothed empirical measures with applications to entropy estimation. *IEEE Transactions on Information Theory*, 66(7):4368–4391.
- Goodfellow, I., Pouget-Abadie, J., Mirza, M., Xu, B., Warde-Farley, D., Ozair, S., Courville, A., and Bengio, Y. (2014). Generative adversarial nets. In *Advances in Neural Information Processing Systems*, pages 2672–2680.

- Hastie, T., Tibshirani, R., and Friedman, J. H. (2009). *The Elements of Statistical Learning: Data Mining, Inference, and Prediction*, volume 2. Springer.
- Heusel, M., Ramsauer, H., Unterthiner, T., Nessler, B., and Hochreiter, S. (2017). GANs trained by a two time-scale update rule converge to a local nash equilibrium. *Advances in Neural Information Processing Systems*, 30.
- Hyvärinen, A. (2005). Estimation of non-normalized statistical models by score matching. *Journal of Machine Learning Research*, 6(Apr):695–709.
- Jain, A. and Poole, B. (2022). Journey to the BAOAB-limit: finding effective MCMC samplers for score-based models. *Workshop on Score-Based Methods at NeurIPS*.
- Krizhevsky, A., Hinton, G., et al. (2009). Learning multiple layers of features from tiny images.
- Miyasawa, K. (1961). An empirical Bayes estimator of the mean of a normal population. *Bulletin of the International Statistical Institute*, 38(4):181–188.
- Parzen, E. (1962). On estimation of a probability density function and mode. *The Annals of Mathematical Statistics*, 33(3):1065–1076.
- Raphan, M. and Simoncelli, E. P. (2011). Least squares estimation without priors or supervision. *Neural Computation*, 23(2):374–420.
- Robbins, H. (1956). An empirical Bayes approach to statistics. In *Proc. Third Berkeley Symp.*, volume 1, pages 157–163.
- Sachs, M., Leimkuhler, B., and Danos, V. (2017). Langevin dynamics with variable coefficients and nonconservative forces: from stationary states to numerical methods. *Entropy*, 19(12):647.
- Saremi, S. and Hyvärinen, A. (2019). Neural empirical Bayes. *Journal of Machine Learning Research*, 20(181):1–23.
- Saremi, S., Mehrjou, A., Schölkopf, B., and Hyvärinen, A. (2018). Deep energy estimator networks. *arXiv preprint arXiv:1805.08306*.
- Saremi, S. and Srivastava, R. K. (2022). Multimeasurement generative models. In *International Conference on Learning Representations*.
- Shannon, C. E. (1948). A mathematical theory of communication. *The Bell System Technical Journal*, 27(3):379–423.
- Shen, R. and Lee, Y. T. (2019). The randomized midpoint method for log-concave sampling. *Advances in Neural Information Processing Systems*, 32.
- Song, Y. and Ermon, S. (2019). Generative modeling by estimating gradients of the data distribution. *arXiv preprint arXiv:1907.05600*.
- Vapnik, V. (1999). *The Nature of Statistical Learning Theory*. Springer Science & Business Media.
- Vincent, P. (2011). A connection between score matching and denoising autoencoders. *Neural Computation*, 23(7):1661–1674.